ACS Medicinal Chemistry Letters

Open Access

This article is licensed under CC-BY 4.0

pubs.acs.org/acsmedchemlett

Letter

Tetraphenylethylene-Based Photoluminescent Self-Assembled Nanoparticles: Preparation and Biological Evaluation

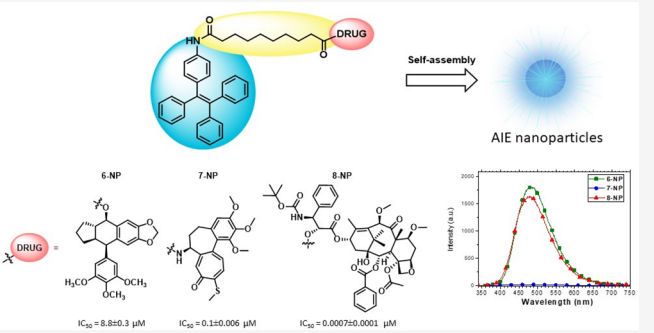
Eleonora Colombo, Elif Merve Aydın, İdil Su Canıtez, Laura Polito, Marta Penconi, Alberto Bossi, Elisa Impresari, Daniele Passarella, Sabrina Dallavalle, Constantinos M. Athanassopoulos, Sara Pellegrino, Irem Durmaz Şahin,* and Michael S. Christodoulou*

Cite This: ACS Med. Chem. Lett. 2023, 14, 1472−1477

Read Online

ACCESS | Metrics & More | Article Recommendations | Supporting Information

ABSTRACT: The conjugation of tetraphenylethylene (TPE) with podophyllotoxin, *N*-desacetylthiocolchicine, and cabazitaxel through a sebacic acid linker led to the formation of fluorescent nanoparticles. Dynamic light scattering (DLS) and photoluminescence spectroscopy were used for the identification and characterization of the fluorescent nanoparticles. The biological evaluation was determined in three human ovarian (KURAMOCHI, OVCAR3, OVSAHO) and three human breast (MCF7, SKBR 3, and MDA-MB231) cancer cell lines. In the case of cabazitaxel, the nanoparticles maintained the activity of the parent drug, at the low nanomolar range, while exhibiting high blue fluorescence. The internalization of the fluorescent NPs into cells was detected using immunofluorescence assay.



KEYWORDS: *Tetraphenylethylene, self-assembled nanoparticles, cancer cell lines, podophyllotoxin, N-desacetylthiocolchicine, cabazitaxel, aggregation-induced emission*

Downloaded via 78.183.134.116 on February 20, 2025 at 10:49:14 (UTC).
See https://pubs.acs.org/sharingguidelines for options on how to legitimately share published articles.

In recent years, nanomedicine has become increasingly more important as a tool to improve the bioavailability of drugs used for the treatment of various diseases, as it can help overcome a range of different issues including low bioavailability due to poor absorption and degradation after reaching the target site.[1]

Our group is particularly interested in a research niche in nanotechnology that is represented by self-assembling drug conjugates able to spontaneously form nanoparticles (NPs) in aqueous media. These conjugates present the same general structure in which the drug is covalently linked to lipophilic moieties, able to induce the structural organization of building blocks because of specific local interactions. This kind of NPs is easy to obtain and can reach high local drug concentrations in tissues, weakening the systemic toxicity of drugs. Over the years, we have reported different constructs, designing conjugates able to release the drug in cellular media,[2−4] hetero-NPs bearing two different drugs,[5−7] and fluorescent hetero-NPs.[5,8] The fundamental moiety of this kind of NPs is the self-assembly inducer that could either be squalene,[2,5,6,8−11] 4-(1,2-diphenylbut-1-en-1-yl) aniline,[3,12,13] 20-hydroxyecdisone,[7] betulinic acid,[14] or cannabidiol.[4] In all cases, the choice of self-assembly inducer is important for the formation of NPs.

We envisage using the 4-amino tetraphenylethylene (TPE) scaffold (**1**, Figure 1) as the self-assembly inducer, a compound

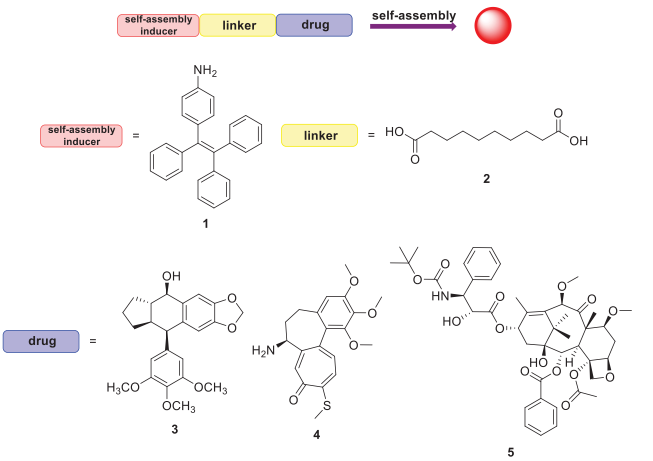


Figure 1. Building blocks of the conjugates.

Received: September 5, 2023
Accepted: September 26, 2023
Published: September 29, 2023



© 2023 The Authors. Published by American Chemical Society

https://doi.org/10.1021/acsmedchemlett.3c00396
ACS Med. Chem. Lett. 2023, 14, 1472−1477

similar to the previously mentioned 4-(1,2-diphenylbut-1-en-1-yl) aniline. Replacement of the ethyl chain with a phenyl ring provides a tetraphenylethylene (TPE) moiety, one of the most promising aggregation-induced emission (AIE) luminophores.[15] AIE is a phenomenon correlated to certain materials that show negligible or extremely weak emission in dilute solution, while they brightly emit in the solid or aggregate state.[16] Due to this interesting behavior, AIEgens have been increasingly applied in the design of materials involving such aggregation states, e.g., nanoparticles.[17] Examples of AIE nanoparticles are present in literature, mainly as diagnostic tools[18,19] but also for drug delivery because of their multiple functions including bioluminescence, drug release monitoring, and low biological toxicity.[17,20,21] Recently, we showed that the conjugation of fatty acids with the 4-amino TPE leads to the formation of supramolecular aggregates that are able to self-assemble into different supramolecular emissive structures depending on the chemical composition and water content.[22] Here, we exploited the same approach in order to obtain emissive self-assembling drug conjugates. This would make possible an easy preparation of fluorescent NPs, an important tool to follow the dynamics of drug internalization.[23,24] For the synthesis of these NPs, three different drugs, podophyllotoxin (**3**), *N*-desacetylthiocolchicine (**4**), and cabazitaxel (**5**), were selected, all of them with the ability to interact with microtubules as stabilizers or destabilizers, connected with sebacic acid (**2**) as the linker[3,11] (Figure 1).

Three different conjugates **6**, **7**, and **8** (Figure 2) were synthesized according to Schemes 1 and 2. A McMurry

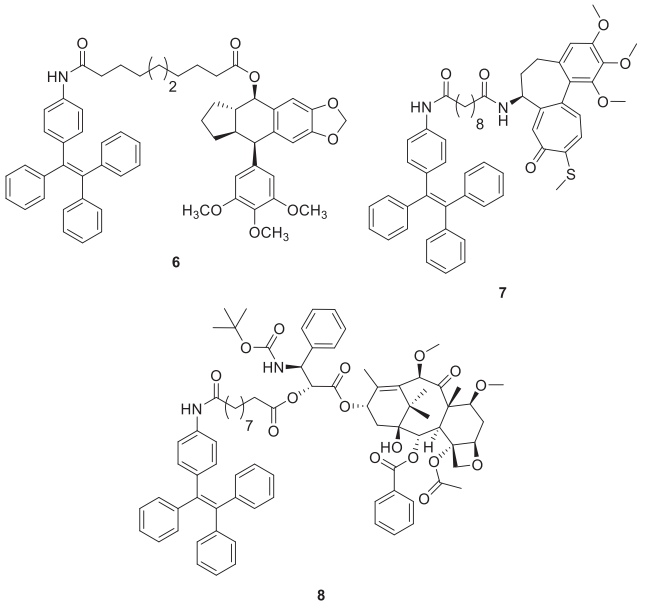
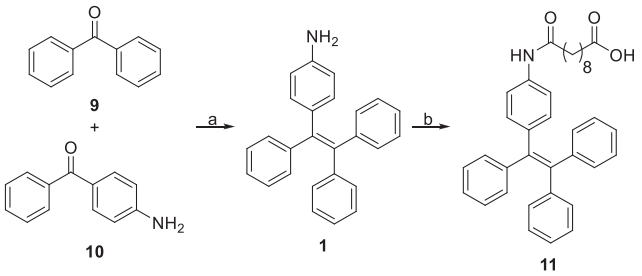


Figure 2. Structures of the obtained conjugates **6**, **7**, and **8**.

coupling[25,26] between benzophenone (**9**) and 4-amino-benzophenone (**10**) furnished the self-assembly inducer 4-(1,2,2-triphenylvinyl) aniline (4-amino TPE) (**1**),[13] which was then condensed with sebacic acid (**2**) to provide the desired intermediate acid **11** (Scheme 1).

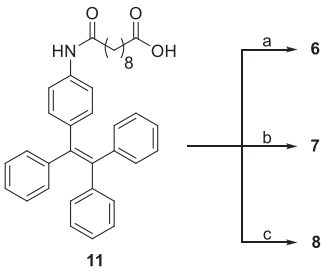
Subsequently, acid **11** was coupled with the appropriate drugs, **3**, **4**, and **5**, in a EDC·HCl/DMAP-mediated condensation reaction for drugs **3** and **5** and HATU/DIPEA-mediated condensation reaction for drug **4** to provide the desired conjugates **6**, **7**, and **8** in good yields (70%, 72%, and

Scheme 1. Synthesis of Intermediate Acid 11[a]



[a]Reagents and conditions: (a) Zn, $TiCl_4$, CH_2Cl_2, −10 °C to reflux; (b) sebacic acid (**2**), DIPEA, HATU, CH_2Cl_2, r.t.

Scheme 2. Synthesis of Conjugates 6−8[a]



[a]Reagents and conditions: (a) **3**, EDC·HCl, DMAP, CH_2Cl_2, r.t., overnight; (b) **4**, HATU, DIPEA, THF, reflux; (c) **5**, EDC·HCl, DMAP, CH_2Cl_2, r.t., overnight.

67%, respectively) (Scheme 2). During the synthesis, no unexpected or unusually high safety hazards were encountered.

The successful nanoparticle formation through solvent evaporation protocol of the conjugates **6**, **7** and **8** was evaluated by dynamic light scattering (DLS) measurements (Table 1). All the compounds, formulated at a 2 mg/mL

Table 1. Hydrodynamic Diameter, Polydispersity Index, and ζ-Potential of Nanoformulated Compounds 6, 7, and 8

compound	hydrodynamic diameter (nm)	polydispersity index (PI)	ζ-potential (mV)
6-NP	151.8 ± 1.5	0.104 ± 0.026	−23.92 ± 1.21
7-NP	244.1 ± 24.6	0.159 ± 0.014	−33.40 ± 0.30
8-NP	574.5 ± 18.8	0.134 ± 0.031	−42.10 ± 0.70

concentration, gave a stable and monodisperse suspension of NPs, characterized by hydrodynamic diameters (HD) in the range of 150−580 nm and a negative ζ -potential lower than −20 mV.

The photoluminescence properties of the nanoparticles dispersed in water were investigated (Table 2 and Figure 3). **6-NP** and **8-NP** showed intense blue fluorescence with quantum yield of 45% and 41%, respectively, and maximum of emission at 480 nm for both, while nanoparticles **7-NP** were not

Table 2. Maximum Emission Wavelength (λ_{em}) and Quantum Yield (φ_{PL}) of Fluorescence from Nanoparticles of Compounds 6, 7, and 8 dispersed in water

compound	λ^{max}_{em} (nm)	φ_{PL} (%)
6-NP	480	45
7-NP	475	<1
8-NP	480	41

https://doi.org/10.1021/acsmedchemlett.3c00396
ACS Med. Chem. Lett. 2023, 14, 1472−1477

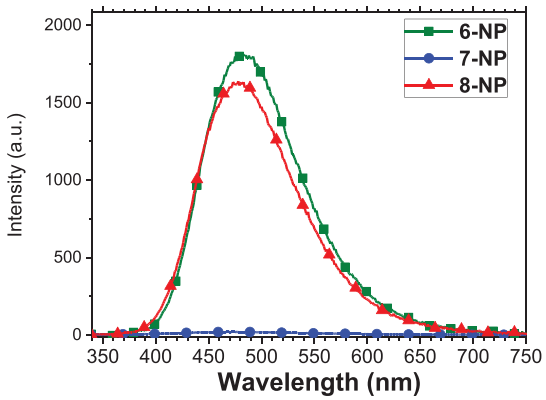


Figure 3. Fluorescence spectra of nanoparticles of conjugates **6**, **7**, and **8** dispersed in water, λ_{ex} = 325 nm.

emissive. For comparison, fluorescence emission has been evaluated in diluted organic solution of the conjugates **6**, **7**, and **8** (EtOH for compound **6** and THF for conjugates **7** and **8**). In this case, all of the compounds displayed negligible fluorescence emission, with quantum yield below 1%. This confirmed the expected behavior of TPE-based molecules with AIE character, which are not emissive as isolated molecules in solution and become highly fluorescent when aggregated as NPs.

The antiproliferative activity of the drugs podophyllotoxin (**3**), *N*-desacetylthiocolchicine (**4**), and cabazitaxel (**5**), of conjugates **6**, **7**, and **8**, their corresponding NPs **6-NP**, **7-NP**, and **8-NP**, and of building block **11** was evaluated in three human ovarian (KURAMOCHI, OVCAR3, OVSAHO) and three human breast (MCF7, SKBR 3, and MDA-MB231) cancer cell lines. The results, expressed as IC_{50} values (nM), are presented in Table 3.

As expected, podophyllotoxin (**3**), *N*-desacetylthiocolchicine (**4**), and cabazitaxel (**5**) were very effective in inducing cytotoxicity in all cell lines, with IC_{50} values in the nanomolar range. On the contrary, the building block **11** did not show any cytotoxicity in all cell lines except for the MCF7 breast cancer cell line, with activity in the high micromolar range (IC_{50} = 42.8 μM). Interestingly, the antiproliferative effects for both conjugates and their NPs was comparable.

In more detail, podophyllotoxin conjugate **6** and its NP **6-NP** showed cell growth inhibition in the low micromolar range in almost all cell lines, with the highest activity in KURAMOCHI and OVCAR3 cell lines, although lower than the parent drug **3**. A similar effect was observed for the drug *N*-desacetylthiocolchicine (**4**) and the conjugate **7** and its NP **7-NP**, the parental drug being very effective in the very low nanomolar range and the conjugates in the very low micromolar range. Note that the IC_{50} values of **7-NP** were in the nanomolar range in all three ovarian cell lines with the highest activity in the OVCAR3 cell line with an IC_{50} value of 100 nM.

The aforementioned differences in order of magnitude between the drug, the conjugate, and its nanoparticle changed in the case of the drug cabazitaxel (**5**). Now, both the conjugate **8** and its NP **8-NP** showed a biological activity closer to the one of the parent drug in almost all cell lines tested, reaching even the low picomolar range (IC_{50} value of 40 pM for **8** on the SKBR 3 cell line). In the KURAMOCHI and MDA-MB231 the conjugate **8** presented higher activity than that of the parent drug. **8-NP** exhibited its highest activity in the OVCAR3 cell line with an IC_{50} value of 700 pM.

For the nanoparticles that presented fluorescence (**6-NP** and **8-NP**), confocal imaging was carried out to investigate the internalization of the nanoparticles inside the cells. OVCAR3 cells were incubated with **6-NP** and **8-NP** for 24 and 48 h and imaged, showing the presence of the fluorescent nanoparticles inside the cells, as shown in Figure 4.

Conclusions. In this paper, we tested the ability of TPE (**1**) to induce the self-assembly of different types of conjugates containing podophyllotoxin (**3**), *N*-desacetylthiocolchicine (**4**), and cabazitaxel (**5**) as drugs. The formation of NPs was confirmed by dynamic light scattering (DLS) measurements. Moreover, in the case of nanoparticles bearing podophyllotoxin (**6-NP**) and cabazitaxel (**8-NP**), high fluorescence in the blue region was detected as a result of the AIE luminogen character of TPE. The not-emissive character of **7-NP** suggests a role of the drug molecule in the AIE behavior of the nanoassembly and evidence the importance of a careful photophysical investigation of these systems.

The synthesized conjugates (**6** and **7**) and their corresponding NPs (**6-NP** and **7-NP**) were tested for their antiproliferative activity in three human ovarian (KURAMOCHI, OVCAR3, OVSAHO) and three human breast (MCF7, SKBR 3, and MDA-MB231) cancer cell lines. Regarding podophyllotoxin and *N*-desacetylthiocolchicine, the conjugates and their NPs displayed very good antiproliferative activity in the μM range and, in some cases, also in the nanomolar range,

Table 3. Cell Growth Inhibition (IC_{50}) of the Compounds and NPs on Human Cancer Cell Lines

	IC_{50} (μM)[a]					
compound	KURAMOCHI	OVCAR3	OVSAHO	MCF7	SKBR 3	MDA-MB231
11	NI[b]	NI[b]	NI[b]	42.8	NI[b]	NI[b]
3	0.0011 ± 0.00003	<0.0001	0.0015 ± 0.0001	0.0001 ± 0.000001	0.00003 ± 0.00002	<0.0001
6	2.3 ± 0.7	7.1 ± 1.6	45.6 ± 7.5	13.7 ± 0.5	10.4 ± 0.4	17.5 ± 2.8
6-NP	24.3 ± 1.7	8.8 ± 0.3	83.7 ± 6.2	22.5 ± 0.9	40.9 ± 0.3.3	35 ± 2.4
4	0.0009 ± 0.0002	<0.0001	0.0037 ± 0.00003	<0.0001	<0.0001	0.2 ± 0.01
7	0.7 ± 0.1	2.0 ± 0.1	12.5 ± 1.9	2.0 ± 0.12	1.1 ± 0.5	2.2 ± 0.13
7-NP	0.8 ± 0.07	0.1 ± 0.006	0.4 ± 0.05	6.3 ± 0.1	8.4 ± 0.4	1.7 ± 0.04
5	0.0018 ± 0.0002	<0.0001	0.0077 ± 0.001	<0.0001	<0.0001	0.0004 ± 0.0001
8	0.0002 ± 0.00006	<0.0001	0.008 ± 0.002	0.0035 ± 0.0002	0.00004 ± 0.00002	0.0002 ± 0.00004
8-NP	0.0393 ± 0.004	0.0007 ± 0.0001	1.065 ± 0.5	0.0073 ± 0.001	0.0013 ± 0.0001	0.0012 ± 0.0004

[a]IC_{50} values are the concentration of tested agent inducing 50% reduction in cell number compared to control cultures after 72 h of incubation. [b]NI = No inhibition.

https://doi.org/10.1021/acsmedchemlett.3c00396
ACS Med. Chem. Lett. 2023, 14, 1472−1477

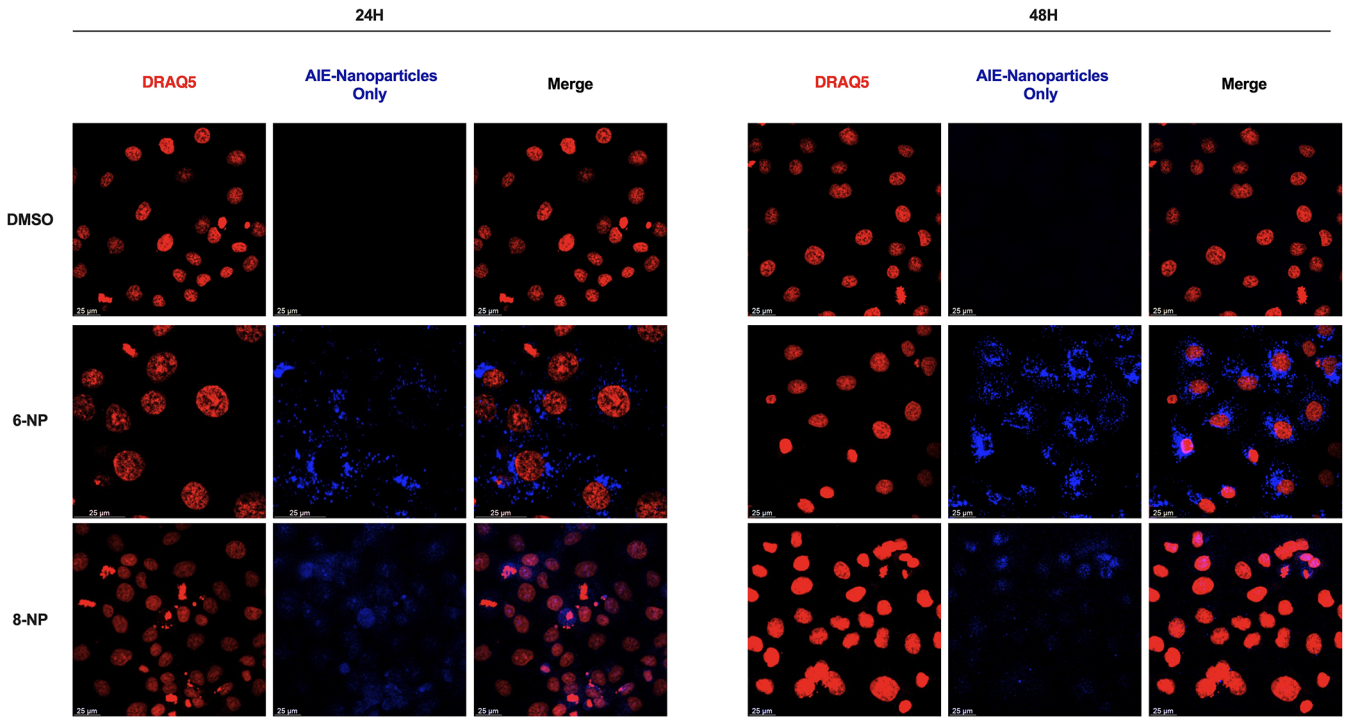


Figure 4. Detection of the internalization of NPs into cells using immunofluorescence assay. Representative images of OVCAR-3 cells after 24 h and 48 h exposure to fluorescent NPs **6-NP** and **8-NP** (Scale bar: 25 μm) (Blue: AEI-Nanoparticles Only, Red: DRAQ5). The nuclei were stained with DRAQ5.

but they were less active than the parent drug in both cases. When cabazitaxel was used as a drug, both the conjugate (**8**) and its corresponding NP (**8-NP**) exhibited antiproliferative activity comparable to the parent drug, and in some cases higher than the drug, reaching even low picomolar activity.

The internalization of the fluorescent NPs into the OVCAR-3 cells was investigated using immunofluorescence assay, showing that said nanoparticles were indeed present inside the cells after treatment.

Our results demonstrated that drug conjugate nanoparticles can be obtained by the use of TPE as self-assembly inducer, and this strategy allows maintaining or even enhancing the antiproliferative capacity of the drug, both as a conjugate and as a NP. In addition, TPE can act as AIE luminogen in promoting the emission of the nanoassemblies, making this system extremely interesting for the study of drug delivery and release by fluorescence techniques.

■ ASSOCIATED CONTENT

Supporting Information

The Supporting Information is available free of charge at https://pubs.acs.org/doi/10.1021/acsmedchemlett.3c00396.

Experimental details for the synthesis of conjugates, preparation and characterization of nanoparticles and biological evaluation (PDF)

■ AUTHOR INFORMATION

Corresponding Authors

Michael S. Christodoulou − *Department of Food, Environmental and Nutritional Sciences (DeFENS), University of Milan, 20133 Milan, Italy;* orcid.org/0000-0002-5098-3143; Email: michail.christodoulou@unimi.it

Irem Durmaz Şahin − *School of Medicine, Koc University, Sariyer, Istanbul 34450, Turkey*; Email: irsahin@ku.edu.tr

Authors

Eleonora Colombo − *Dipartimento di Chimica, Universitá degli Studi di Milano, 20133 Milano, Italy; Ann Romney Center for Neurologic Diseases, Department of Neurology, Brigham and Women's Hospital and Harvard Medical School, Boston, Massachusetts 02115, United States;* orcid.org/0000-0001-9062-4850

Elif Merve Aydın − *Koc University Research Center for Translational Medicine (KUTTAM), Sariyer, Istanbul 34450, Turkey*

İdil Su Canıtez − *Koc University Research Center for Translational Medicine (KUTTAM), Sariyer, Istanbul 34450, Turkey*

Laura Polito − *Istituto di Scienze e Tecnologie Chimiche "Giulio Natta", SCITEC−CNR, 20138 Milano, Italy;* orcid.org/0000-0002-7756-2365

Marta Penconi − *Istituto di Scienze e Tecnologie Chimiche "Giulio Natta", SCITEC−CNR, 20138 Milano, Italy; SmartMatLab Center, 20133 Milano, Italy;* orcid.org/0000-0001-7459-7354

Alberto Bossi − *Istituto di Scienze e Tecnologie Chimiche "Giulio Natta", SCITEC−CNR, 20138 Milano, Italy; SmartMatLab Center, 20133 Milano, Italy*

Elisa Impresari − *DISFARM, Dipartimento di Scienze Farmaceutiche, Sezione Chimica Generale e Organica "A. Marchesini", Università degli Studi di Milano, 20133 Milano, Italy*

Daniele Passarella − *Dipartimento di Chimica, Universitá degli Studi di Milano, 20133 Milano, Italy*

https://doi.org/10.1021/acsmedchemlett.3c00396
ACS Med. Chem. Lett. 2023, 14, 1472−1477

Sabrina Dallavalle − *Department of Food, Environmental and Nutritional Sciences (DeFENS), University of Milan, 20133 Milan, Italy;* orcid.org/0000-0002-8813-8922

Constantinos M. Athanassopoulos − *Synthetic Organic Chemistry Laboratory, Department of Chemistry, University of Patras, GR-26504 Patras, Greece;* orcid.org/0000-0002-7549-1911

Sara Pellegrino − *DISFARM, Dipartimento di Scienze Farmaceutiche, Sezione Chimica Generale e Organica "A. Marchesini", Università degli Studi di Milano, 20133 Milano, Italy;* orcid.org/0000-0002-2325-3583

Complete contact information is available at: https://pubs.acs.org/10.1021/acsmedchemlett.3c00396

Author Contributions

The manuscript was written through contributions of all authors. All authors have given approval to the final version of the manuscript.

Notes

The authors declare no competing financial interest.

■ ACKNOWLEDGMENTS

This work was supported by Koç University School of Medicine. The authors gratefully acknowledge the use of the services and facilities of the Koç University Research Center for Translational Medicine (KUTTAM), funded by the Presidency of Turkey, Presidency of Strategy and Budget and Progetto Integrato Regione Lombardia and Fondazione CARIPLO (grant numbers 12689/13, 7959/13; Azione 1 e 2, "SmartMatLab centre" and Fondazione CARIPLO grant 2013-1766).

■ ABBREVIATIONS

AIE, aggregation-induced emission; DIPEA, *N*,*N*-diisopropylethylamine; DMAP, 4-dimethylaminopyridine; EDC·HCl, *N*-ethyl-*N*′-(3-dimethylaminopropyl) carbodiimide hydrochloride; HATU, 1-[bis(dimethylamino) methylene]-1*H*-1,2,3-triazolo[4,5-*b*]pyridinium 3-oxid hexafluorophosphate; NPs, nanoparticles; THF, tetrahydrofuran; TPE, tetraphenylethylene

■ REFERENCES

(1) Zhang, C.; Yan, L.; Wang, X.; Zhu, S.; Chen, C.; Gu, Z.; Zhao, Y. Progress, Challenges, and Future of Nanomedicine. *Nano Today* **2020**, *35*, 101008.

(2) Borrelli, S.; Christodoulou, M. S.; Ficarra, I.; Silvani, A.; Cappelletti, G.; Cartelli, D.; Damia, G.; Ricci, F.; Zucchetti, M.; Dosio, F.; Passarella, D. New Class of Squalene-Based Releasable Nanoassemblies of Paclitaxel, Podophyllotoxin, Camptothecin and Epothilone A. *Eur. J. Med. Chem.* **2014**, *85*, 179−190.

(3) Fumagalli, G.; Polito, L.; Colombo, E.; Foschi, F.; Christodoulou, M. S.; Galeotti, F.; Perdicchia, D.; Bassanini, I.; Riva, S.; Seneci, P.; García-Argáez, A.; Dalla Via, L.; Passarella, D. Self-Assembling Releasable Thiocolchicine-Diphenylbutenylaniline Conjugates. *ACS Med. Chem. Lett.* **2019**, *10* (4), 611−614.

(4) Colombo, E.; Coppini, D. A.; Polito, L.; Ciriello, U.; Paladino, G.; Hyeraci, M.; Di Paolo, M. L.; Nordio, G.; Dalla Via, L.; Passarella, D. Cannabidiol as Self-Assembly Inducer for Anticancer Drug-Based Nanoparticles. *Molecules* **2023**, *28* (1), 112.

(5) Fumagalli, G.; Mazza, D.; Christodoulou, M. S.; Damia, G.; Ricci, F.; Perdicchia, D.; Stella, B.; Dosio, F.; Sotiropoulou, P. A.; Passarella, D. Cyclopamine-Paclitaxel-Containing Nanoparticles: Internalization in Cells Detected by Confocal and Super-Resolution Microscopy. *ChemPlusChem.* **2015**, *80* (9), 1380−1383.

(6) Fumagalli, G.; Stella, B.; Pastushenko, I.; Ricci, F.; Christodoulou, M. S.; Damia, G.; Mazza, D.; Arpicco, S.; Giannini, C.; Morosi, L.; Dosio, F.; Sotiropoulou, P. A.; Passarella, D. Heteronanoparticles by Self-Assembly of Doxorubicin and Cyclopamine Conjugates. *ACS Med. Chem. Lett.* **2017**, *8* (9), 953−957.

(7) Fumagalli, G.; Giorgi, G.; Vágvölgyi, M.; Colombo, E.; Christodoulou, M. S.; Collico, V.; Prosperi, D.; Dosio, F.; Hunyadi, A.; Montopoli, M.; Hyeraci, M.; Silvani, A.; Lesma, G.; Via, L. D.; Passarella, D. Heteronanoparticles by Self-Assembly of Ecdysteroid and Doxorubicin Conjugates to Overcome Cancer Resistance. *ACS Med. Chem. Lett.* **2018**, *9* (5), 468−471.

(8) Borrelli, S.; Cartelli, D.; Secundo, F.; Fumagalli, G.; Christodoulou, M. S.; Borroni, A.; Perdicchia, D.; Dosio, F.; Milla, P.; Cappelletti, G.; Passarella, D. Self-Assembled Squalene-Based Fluorescent Heteronanoparticles. *ChemPlusChem.* **2015**, *80* (1), 47−49.

(9) Frapporti, G.; Colombo, E.; Ahmed, H.; Assoni, G.; Polito, L.; Randazzo, P.; Arosio, D.; Seneci, P.; Piccoli, G. Squalene-Based Nano-Assemblies Improve the Pro-Autophagic Activity of Trehalose. *Pharmaceutics* **2022**, *14* (4), 862.

(10) Colombo, E.; Biocotino, M.; Frapporti, G.; Randazzo, P.; Christodoulou, M. S.; Piccoli, G.; Polito, L.; Seneci, P.; Passarella, D. Nanolipid-Trehalose Conjugates and Nano-Assemblies as Putative Autophagy Inducers. *Pharmaceutics* **2019**, *11* (8), 422.

(11) Ntungwe, E.; Domínguez-Martín, E. M.; Bangay, G.; Garcia, C.; Guerreiro, I.; Colombo, E.; Saraiva, L.; Díaz-Lanza, A. M.; Rosatella, A.; Alves, M. M.; Reis, C. P.; Passarella, D.; Rijo, P. Self-Assembly Nanoparticles of Natural Bioactive Abietane Diterpenes. *Int. J. Mol. Sci.* **2021**, *22* (19), 10210.

(12) Fumagalli, G.; Christodoulou, M. S.; Riva, B.; Revuelta, I.; Marucci, C.; Collico, V.; Prosperi, D.; Riva, S.; Perdicchia, D.; Bassanini, I.; García-Argáez, A.; Via, L. D.; Passarella, D. Self-Assembled 4-(1,2-Diphenylbut-1-En-1-Yl) Aniline Based Nanoparticles: Podophyllotoxin and Aloin as Building Blocks. *Org. Biomol Chem.* **2017**, *15* (5), 1106−1109.

(13) Colombo, E.; Coppini, D. A.; Maculan, S.; Seneci, P.; Santini, B.; Testa, F.; Salvioni, L.; Vanacore, G. M.; Colombo, M.; Passarella, D. Folic Acid Functionalization for Targeting Self-Assembled Paclitaxel-Based Nanoparticles. *RSC Adv.* **2022**, *12* (54), 35484−35493.

(14) Colombo, E.; Polito, L.; Biocotino, M.; Marzullo, P.; Hyeraci, M.; Via, L. D.; Passarella, D. New Class of Betulinic Acid-Based Nanoassemblies of Cabazitaxel, Podophyllotoxin, and Thiocolchicine. *ACS Med. Chem. Lett.* **2020**, *11* (5), 895−898.

(15) Feng, H.-T.; Yuan, Y.-X.; Xiong, J.-B.; Zheng, Y.-S.; Tang, B. Z. Macrocycles and Cages Based on Tetraphenylethylene with Aggregation-Induced Emission Effect. *Chem. Soc. Rev.* **2018**, *47* (19), 7452−7476.

(16) Luo, J.; Xie, Z.; Lam, J. W. Y.; Cheng, L.; Tang, B. Z.; Chen, H.; Qiu, C.; Kwok, H. S.; Zhan, X.; Liu, Y.; Zhu, D. Aggregation-Induced Emission of 1-Methyl-1,2,3,4,5-Pentaphenylsilole. *Chem. Commun.* **2001**, No. 18, 1740−1741.

(17) Pei, Y.; Wang, Z.; Wang, C. Recent Progress in Polymeric AIE-Active Drug Delivery Systems: Design and Application. *Mol. Pharmaceutics* **2021**, *18* (11), 3951−3965.

(18) Nicol, A.; Qin, W.; Kwok, R. T. K.; Burkhartsmeyer, J. M.; Zhu, Z.; Su, H.; Luo, W.; Lam, J. W. Y.; Qian, J.; Wong, K. S.; Tang, B. Z. Functionalized AIE Nanoparticles with Efficient Deep-Red Emission, Mitochondrial Specificity, Cancer Cell Selectivity and Multiphoton Susceptibility. *Chem. Sci.* **2017**, *8* (6), 4634−4643.

(19) Fan, X.; Xia, Q.; Zhang, Y.; Li, Y.; Feng, Z.; Zhou, J.; Qi, J.; Tang, B. Z.; Qian, J.; Lin, H. Aggregation-Induced Emission (AIE) Nanoparticles-Assisted NIR-II Fluorescence Imaging-Guided Diagnosis and Surgery for Inflammatory Bowel Disease (IBD). *Adv. Healthc Mater.* **2021**, *10* (24), 2101043.

(20) Li, J.; Lee, M. M. S.; Li, H.; Tong, C.; Huang, J.; Yan, Y.; Wang, D.; Tang, B. Z. Programmed Self-Assembly of Protein-Coated AIE-Featured Nanoparticles with Dual Imaging and Targeted Therapy to Cancer Cells. *ACS Appl. Mater. Interfaces* **2020**, *12*, 29641.

(21) Yuan, Y.; Xu, S.; Zhang, C. J.; Liu, B. Light-Responsive AIE Nanoparticles with Cytosolic Drug Release to Overcome Drug Resistance in Cancer Cells. *Polym. Chem.* **2016**, *7* (21), 3530−3539.
(22) Impresari, E.; Bossi, A.; Lumina, E. M.; Ortenzi, M. A.; Kothuis, J. M.; Cappelletti, G.; Maggioni, D.; Christodoulou, M. S.; Bucci, R.; Pellegrino, S. Fatty Acids/Tetraphenylethylene Conjugates: Hybrid AIEgens for the Preparation of Peptide-Based Supramolecular Gels. *Front Chem.* **2022**, *10*. DOI: 10.3389/fchem.2022.927563.
(23) Ruedas-Rama, M. J.; Walters, J. D.; Orte, A.; Hall, E. A. H. Fluorescent Nanoparticles for Intracellular Sensing: A Review. *Anal. Chim. Acta* **2012**, *751*, 1−23.
(24) Zalmi, G. A.; Jadhav, R. W.; Mirgane, H. A.; Bhosale, S. v. Recent Advances in Aggregation-Induced Emission Active Materials for Sensing of Biologically Important Molecules and Drug Delivery System. *Molecules* **2022**, *27* (1), 150.
(25) Christodoulou, M. S.; Fokialakis, N.; Passarella, D.; García-Argáez, A. N.; Gia, O. M.; Pongratz, I.; Dalla Via, L.; Haroutounian, S. A. Synthesis and Biological Evaluation of Novel Tamoxifen Analogues. *Bioorg. Med. Chem.* **2013**, *21* (14), 4120−4131.
(26) Christodoulou, M. S.; Zarate, M.; Ricci, F.; Damia, G.; Pieraccini, S.; Dapiaggi, F.; Sironi, M.; lo Presti, L.; García-Argáez, A. N.; Dalla Via, L.; Passarella, D. 4-(1,2-Diarylbut-1-En-1-Yl) Isobutyranilide Derivatives as Inhibitors of Topoisomerase II. *Eur. J. Med. Chem.* **2016**, *118*, 79−89.

https://doi.org/10.1021/acsmedchemlett.3c00396
ACS Med. Chem. Lett. 2023, 14, 1472−1477